

1

2

3

4

5

6

7

8 An Inexpensive Smartphone-Based Device and Predictive Models for Rapid, Non-Invasive, and Point-of-Care Monitoring

9 of Ocular and Cardiovascular Complications Related to Diabetes

10

11 Kasyap Chakravadhanula<sup>1</sup>

12 1 - BASIS Scottsdale, 10400 N 128th St, Scottsdale, AZ 85259

13 Corresponding Author: Kasyap Chakravadhanula, (480)-825-6678

14

15

16

17

18

19

20

21

NOTE: This preprint reports new research that has not been certified by peer review and should not be used to guide clinical practice.

22

23 **Abstract**

24 Diabetes is a massive global problem, with growth especially rapid in developing regions, which can lead to several  
25 damaging complications. Among the most impactful of these are diabetic retinopathy, the leading cause of blindness  
26 among working class adults, and cardiovascular disease, the leading cause of death worldwide. However, diagnosis is  
27 often too late to prevent irreversible damage caused by these linked conditions. This study describes the development of  
28 an integrated test, automated and not requiring laboratory blood analysis, for screening of these conditions. First, a random  
29 forest model was developed by retrospectively analyzing the influence of various risk factors (obtained quickly and non-  
30 invasively) on cardiovascular risk. Next, a deep-learning model was developed for prediction of diabetic retinopathy from  
31 retinal fundus images by a modified and re-trained InceptionV3 image classification model. The input was simplified by  
32 automatically segmenting the blood vessels in the retinal image. The technique of transfer learning enables the model to  
33 capitalize on existing infrastructure on the target device, meaning more versatile deployment, especially helpful in low-  
34 resource settings. The models were integrated into a smartphone-based device, combined with an inexpensive 3D-printed  
35 retinal imaging attachment. Accuracy scores, as well as the receiver operating characteristic curve, the learning curve, and  
36 other gauges, were promising. This test is much cheaper and faster, enabling continuous monitoring for two damaging  
37 complications of diabetes. It has the potential to replace the manual methods of diagnosing both diabetic retinopathy and  
38 cardiovascular risk, which are time consuming and costly processes only done by medical professionals away from the  
39 point of care, and to prevent irreversible blindness and heart-related complications through faster, cheaper, and safer  
40 monitoring of diabetic complications. As well, tracking of cardiovascular and ocular complications of diabetes can enable  
41 improved detection of other diabetic complications, leading to earlier and more efficient treatment on a global scale.

42 *Keywords: Diabetic Retinopathy Screening, Smartphone Ophthalmology, Cardiovascular Risk, Point-of-Care Screening,*  
43 *Machine Learning, Computer Vision*

---

44

45 **1. Introduction**

46 Approximately four hundred and twenty million people worldwide have been diagnosed with diabetes mellitus, and this is  
47 predicted only to increase. Of those with diabetes, approximately one-third are expected to be diagnosed with diabetic  
48 retinopathy (DR), a chronic eye disease that can progress to irreversible vision loss, and the leading cause of blindness  
49 among working-class individuals (Facts About Diabetic Eye Disease, 2015). Early detection, which is vital for effective  
50 prognosis, relies on skilled readers and is both labor and time-intensive, which limits who can be helped. Skilled readers  
51 perform prognosis by analysis of swelling in the retina that threatens vision, of evidence of poor retinal blood vessel  
52 circulation, or of abnormal vessels or tissue in the retina [4]. Moreover, the manual nature of DR screening methods  
53 creates inconsistency among readers [4].

54

55 Xie et al. [15] found that patients with proliferative diabetic retinopathy have an increased risk of incident cardiovascular  
56 disease (which can manifest in abnormalities in ocular blood vessels), meaning that these patients must be followed up  
57 with more closely to prevent cardiovascular disease. Due to this connection, simultaneous monitoring has several  
58 advantages to improve early detection and risk prediction of incident cardiovascular disease.

59

60 Cardiovascular disease is the leading cause of death in the world, for both men and women. In the U.S., 1 in every 4  
61 deaths is due to cardiovascular disease. Although cardiovascular disease is a leading cause of deaths globally, many do not  
62 act on risk factors and warning signs although about half (47%) of Americans have at least one significant risk factor [7].

---

63

64 For these extremely prevalent problems, current methods (detailed below) of risk detection/prediction are costly, slow,  
65 inaccessible, and often inconsistent. Due to the emergence of more accessible machine learning, machine learning and  
66 deep learning are being applied to various medical problems as well. Thus far application of these methods to automate  
67 prediction of diabetic retinopathy and cardiovascular risk, while accurate, have been resource-intensive and  
68 computationally costly, creating an inability to apply these methods on devices in low-resource settings. As well, these  
69 tests have been separated (see “Discussion” section for further comparison). This study aimed to apply various machine  
70 learning/deep learning algorithms to more cheaply, quickly, accessibly, and consistently monitor diabetic retinopathy and  
71 cardiovascular disease in a comprehensive test.

72 A recent publication by EyePACS [3] revealed the use of retinal fundus images in the prediction of diabetic retinopathy.  
73 Research has shown that many other aspects of health may be predicted via the analysis of retinal fundus images (age, sex,  
74 systolic BP, and smoker % among others), which are all risk factors of cardiovascular disease.

75 Although there exist fairly accurate automated tests to predict groups at risk of cardiovascular disease (for example Pooled  
76 Cohort and Framingham), these tests are time-consuming, resource-intensive, and invasive. This is due to the fact that  
77 several risk factors in the analysis are determined in a blood test, which often take much time to return results, are costly,  
78 and are often not available in low-resource areas [11, 12]. For this reason, the current method of assessing cardiovascular  
79 risk is not suitable for effective continuous monitoring on a large scale. The gap for a more accessible and easily  
80 performable test is the one this study desired to fill, by creating a smartphone-based, easily administered test through the  
81 analysis of both risk factors (via user input) and of retinal fundus images.

---

82 Current methods of diagnosing diabetic retinopathy (D.R.) require a retinal fundus image which must be taken in a  
83 properly equipped facility by a trained professional using a device that can cost ~\$5,000. The image must then be  
84 processed by a professional reader, which is very time-consuming (up to 7 weeks). The current method is slow,  
85 inconvenient, expensive, and inconsistent (due to manual reading), and is thus ineffective for early detection and response  
86 before damage is irreversible [4]. In developing nations, where diabetic retinopathy is most damaging, the current solution  
87 cannot be implemented effectively.

88 Currently, there exist solutions to automate prediction of diabetic retinopathy from retinal fundus images via deep learning  
89 [4, 14], however current approaches either falter in accuracy or are too computationally resource intensive to be  
90 implemented on most mobile devices (see Discussion section for further explanation).

91 This study sought to construct an inexpensive, convenient, and consistent device for rapid retinal imaging and diagnosis,  
92 which can also be implemented effectively in low-resource settings. Two specific goals of this study are high accuracy in  
93 the prediction of cardiovascular risk without incorporating features that require laboratory blood analysis to determine,  
94 and a computationally light infrastructure leveraging existing models on the smartphone to enable both rapid and complex  
95 analysis on a mobile device. These are especially relevant in low resource settings (implementation in these settings with  
96 regard to adoption and technology availability is discussed further in “Conclusions”).

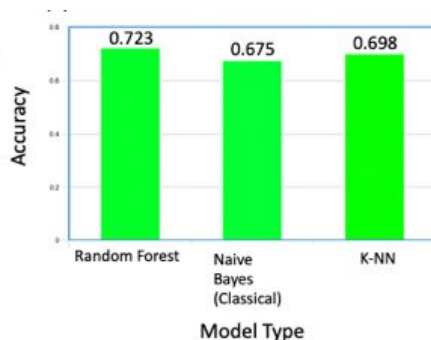
97 Because cardiovascular disease accounts for 1 in 3 deaths in the US [7], and diabetic retinopathy is a leading cause of  
98 vision impairment and blindness worldwide [8], this study has enormous potential for societal impact.

## 99 **2. Materials and Methods**

### 100 **2.1 Cardiovascular Risk Factors Model**

---

101 Eleven input features (which could be taken non-invasively, quickly, and easily) and one output feature (the risk  
102 classification) were chosen from the University of California Irvine (UCI) Heart Disease Dataset [9]). The raw data came  
103 in the form of a spaced list of numbers, with random indents. VBA allowed this data to be structured in a .csv file. The  
104 final step was to use Pandas to convert the .csv to a python NumPy array, which could be used in the model. The “SciKit-  
105 learn” library was used to build models for this task. In order to choose a model structure, the pre-optimization testing  
106 accuracies (using the default parameters from Sci-Kit Learn) of several model types versatile on relatively small datasets  
107 were measured. Accuracy was measured by randomly isolating 20% of the dataset, allowing the model to train on the  
108 remaining 80%, and measuring the classification accuracy of the model on the 20% left for testing samples which the  
109 model had not yet seen. The 3 top performing structures (Random Forest, Classical Naive Bayes, K-Nearest Neighbors)  
110 are compared in Figure 1. The accuracy of the Random Forest model in this preliminary test was the highest, so the  
111 Random Forest Model was chosen for this task. The other models (Naïve Bayes, K-NN) were the 2<sup>nd</sup> and 3<sup>rd</sup> highest  
112 performing models and are depicted only for the sake of comparison; they have no further role in this study.



113  
114 **Figure 1.** The accuracies of Random Forest, Classical Naïve Bayes, and K-Nearest Neighbor compared. Using a “voting”  
115 system, random forest classifiers can quickly learn on data and accurately validate predictions, leading to a higher  
116 efficiency and end performance.

117

---

118 The dataset was split randomly into training and testing sets (20% for testing, the rest is left for training). The optimized  
119 model was built in python with the “SciKit-learn” library and used n=100 estimators (the tree “nodes”), arrived at through  
120 iterative testing of each model in a range of 600 values of n. To measure the optimized testing accuracy of the model in a  
121 low-bias manner, the technique of k-fold cross validation was used. This technique creates k unique sets of training and  
122 testing data (where k is an integer, meaning the number of folds). To evaluate this model, k=10 folds were created,  
123 meaning 10 untrained copies of the model were trained and tested on unique, randomized splits of the original dataset.  
124 Over these 10 folds, the model structure reached an overall test accuracy of ~82%, which was higher than the goal  
125 accuracy and is comparable to other similar tests (discussed further in Discussion section).

## 126 **2.2 Diabetic Retinopathy Model**

127 Transfer Learning is the retraining of the final layers of a pre-trained and tested complex deep learning network, which  
128 results in a comparable accuracy, efficiency, and loss, to building the model from scratch. It requires much less training  
129 data, computational power, model size, and training time.

130 The pretrained model chosen was Inception v3, which showed higher preliminary accuracies than model structures as  
131 VGG and MobileNet. Inception v3 is a model trained to recognize images of 1000 different objects (classes). In transfer  
132 learning, the final “output” layer was retrained to return diagnosis of diabetic retinopathy via Google’s Tensorflow.

133 The dataset chosen was the EYEPacs retinal fundus image dataset [13], a widely-used dataset published as part of an open  
134 competition which contains about 45,000 retinal fundus images and their corresponding grades.

135 Due to the complexity of the eye, our initial approaches to feed the raw images into a transfer deep learning network  
136 yielded low accuracies of below 60%, indicating need for revision.

---

137 Medically, experts diagnose diabetic retinopathy and other conditions in the eye through the observation of blood vessels.

138 So, the model can safely treat all but the blood vessels as “noise” for the identification of diabetic retinopathy. To simplify

139 the input data and remove this “noise,” automatic vessel segmentation was used.

140 To validate the improvement that automatic vessel segmentation could have, the transfer learning model was tested on the

141 DRIVE database [2], which has images which were manually vessel segmented and their corresponding diagnosis of

142 diabetic retinopathy (graded by medical professionals). The model reported accuracy scores of almost 97%, showing the

143 potential of this method.

144 However, the problem which still remained was the automatic “conversion” of retinal fundus images to segmented ones.

145 Due to the complexity of the problem and the plethora of research already done on the many existing datasets, an open

146 source contrast model (like that described in [1]) was transfer learned for this task on parts of the STARE database [6].

147 This model was tested on the datasets DRIVE [2], STARE [6], and HRF [5], which combined have hundreds of image

148 pairs. The model’s predictions closely mirrored the segmented images.

149 There is a visible bias for the lower values in the dataset because the higher levels are just much rarer in the world.

150 However, if one class is overrepresented, especially in deep learning, the model can overfit and predict in accordance with

151 the dataset rather than the image content.

152 A solution is increasing the number of data points at the higher levels. This is achieved by conducting data augmentation.

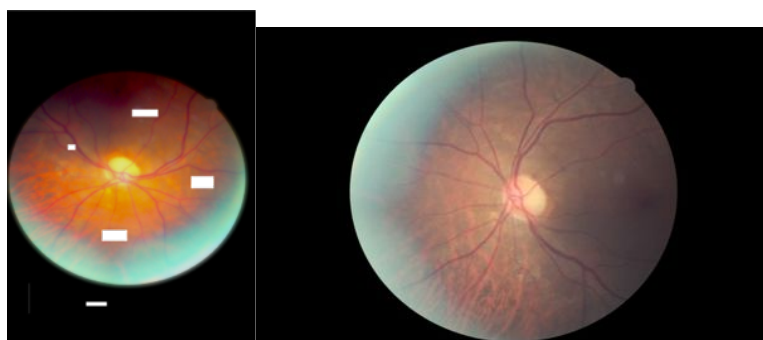
153 Simple data augmentation is the inversion of images or the addition of noise to create new data and also create model

154 “tolerance” for distortion. This was performed for the 3/4 class images through a simple python script. Figure 2 shows the

155 effect of data augmentation on a fundus image.

---

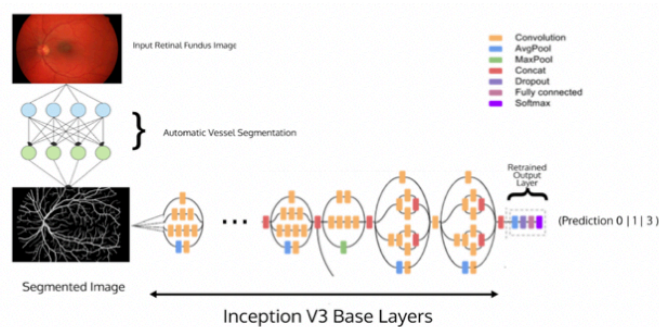




156

157 **Figure 2.** Left – Original Retinal Fundus Image, Right – Augmented Retinal Fundus Image with orientation changed,  
158 distortion added, alpha and relative exposure changed, and spots removed (Retinal Image from EYEPacs Dataset in [13],  
159 described above).

160 The final model architecture is shown in Figure 3.



161

162 **Figure 3.** Final Model Architecture, with Automatic Vessel Segmentation and Inceptionv3 transfer learning. The model,  
163 when tested on the EYEPACS dataset using the 10-fold cross validation method described earlier, recorded a testing  
164 accuracy of ~81%, which is highly respectable (see Discussion section for further comparison).

### 165 2.3 Smartphone Implementation and Prototype

166 The App and User Interface were coded/designed in the IDE XCode, in the Swift language.

167 Since the models were written in languages and with libraries not iOS native, the models were converted to CoreML, the  
168 iOS native construction for machine learning, using another library called coremltools. After this conversion, the app  
169 could make full use of the models. The next step was designing a professional and clean User Interface (UI) and User  
170 Experience (UX), which was achieved using the versatile XCode IDE.

171 While each individual model had been tested, the comprehensive test had yet to be evaluated.

172 The model was tested in multiple trials, on 50 random data collections from the UCI Heart Disease Dataset (each data  
173 collection consists of 12 values – 11 risk factors and 1 risk value). The UCI Heart Disease Dataset does not include retinal  
174 fundus images, so an image from the EyePACS dataset was inputted based on the D.R. classification of severity in the  
175 UCI collection.

176 Overall, the test had an accuracy of 80% over 50 collections. When the classification was made binary for each model, as  
177 it will likely be in a real-world implementation, the accuracy was 96%.

178 Because retinal fundus images are typically taken on an expensive and immobile machine (see Figure 4), a more mobile  
179 and cheaper version needed to be developed to fit the smartphone application.



180

181 **Figure 4.**Traditional Retinal Imaging Machines, costing around \$5,000.

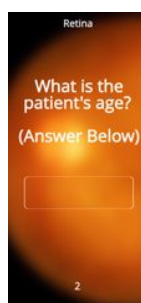
---

182 For this purpose, a 3D-printed smartphone attachment was designed and built. This attachment fits to the smartphone  
183 camera and is adjustable. As well, it is lightweight, compact, user-friendly (with some basic instruction), versatile, and  
184 inexpensive (about 100 times lower cost). The attachment can use the phone's native flash for lighting or any other  
185 coaxial light source.



186

187 **Figure 5.** The left image shows the device camera view from a retinal fundus image (device tested on and image taken  
188 from real retina, background replaced with white). The right image shows the 3D-printed device fitted to the smartphone,  
189 which is the device configuration (lens was removed).



190

191 **Figure 6.** The app takes some basic risk factors as input for the models.

## 192 2.4 Evaluation

193 Although an important way to gauge model performance is simply model accuracy, there are several other, more  
194 descriptive ways to do so which ensure the model performs on multiple fronts.

---

195 **Receiver Operating Characteristic (ROC) curve**

196 ROC curves show the ability of a model to distinguish between classes. An ROC curve is created by varying the threshold  
197 between classifications and measuring the “True” or correct positive portion versus the “false” or incorrect positive  
198 portion. A good ROC curve means that the “overlap” between the classes is small (or the model is more “sure” in its  
199 predictions), especially important in medical computing problems.

200 The distance between the ROC curve and the centerline signifies the amount of distinctness the model assigns to each  
201 class (a high distance is more “sureness” and less class overlap).

202 In an ROC curve, the AUC ROC (Area under the ROC curve) is the best measure of model performance. An excellent  
203 model has an AUC ROC near to 1 (a horizontal line at TPR = 1), meaning it has a very high measure of separability. A  
204 poor model has an AUC ROC near to 0 (a horizontal line at TPR = 0), meaning it has the worst measure of separability.  
205 When the AUC ROC = 0.5, the model has no distinctive capability.

206 **Learning Curve (Test and Training Accuracies against Proportion of Data Set)**

207 A learning curve is a visualization of how training and test accuracies vary when the size of the dataset changes, as the  
208 model gains more experience. The learning curve is useful in that it shows how adding more data may or may not benefit  
209 the model, telling the researcher if pursuing more data will in fact be useful. It also is an indicator of overfitting and  
210 underfitting. The learning curves for both models are below (Figure 8).

211 The most important performance measure discerned from the learning curve is fit. There are two possible problems related  
212 to fit: overfit and underfit.

---

213 Overfit occurs when a model's predictive ability corresponds too closely to a particular dataset and may therefore fail to  
214 fit additional data or generalize to future observations reliably. Overfit is analytically when accuracy substantially drops  
215 with new data, such as in the testing set. If the curve for training (red) is not convergent with the testing line (green), the  
216 model has overfit, because the testing accuracy will never reach the training accuracy even with a large enough dataset.

217 In addition, if the curves greatly reduce in concavity with higher and higher values, the model is struggling to generalize  
218 to more data and noise, which is underfit.

## 219 **Feature Importance**

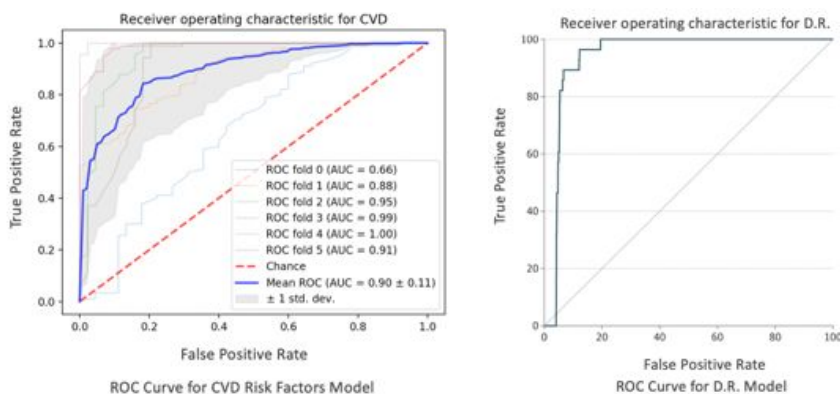
220 Feature importance is an important visualization for models with a possible medical application, largely because both  
221 physicians and patients need to trust the model, and also because feature importance analysis can reveal new insight on the  
222 condition or biological system. This graph can be used to inform patients and physicians about why the model made a  
223 specific prediction and to inform patients how to improve their risk classification, with the most important risk factors  
224 being age, rest heart rate, and classification of severity of diabetic retinopathy.

## 225 **3. Results**

### 226 **3.1 Receiver Operating Characteristic (ROC) curve**

227 Figure 7 shows the Receiver Operating Characteristic (ROC) curves for each model.

---



228

229 **Figure 7.** ROC curves for each model. The independent variable is the threshold value, and the dependent variable is the  
 230 relationship between TPR and FPR.

231 The Mean AUC ROC (in 5-fold cross validation) of the cardiovascular risk factors model was 0.90 with 95% C.I. +/-

232 0.11, and the Mean AUC ROC (also in 5-fold cross validation) of the diabetic retinopathy model was 0.982 with 95% C.I.

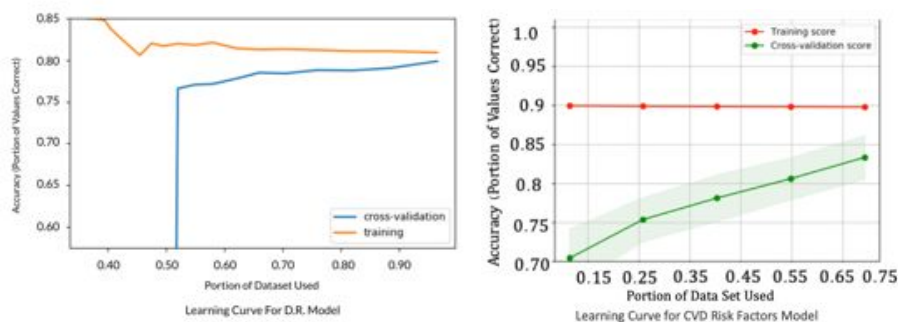
233 +/- 0.002.

234 Note: The data was dichotomized for this curve (because of the nature of the ROC measuring two-class distinction), so

235 these curves demonstrate the models' distinction purely between at risk or not at risk.

### 236 3.2 Learning Curve

237 Figure 8 shows the Learning Curve for each model.



238

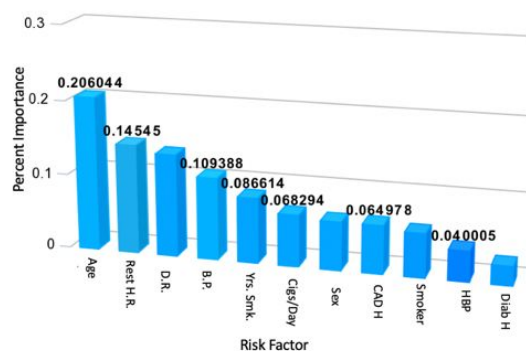
239 **Figure 8.** Learning curves for each model, with training indicated by the red curve (orange for D.R. model) and testing or  
240 cross-validation by the green (blue for the D.R. model). The independent variable is the data set portion, and the  
241 dependent variable is accuracy.

242 For the cardiovascular risk factors model, the shared point of convergence with more data shows the growth potential with  
243 more data. The cap is about 90%, which is extremely well-performing. With the dataset at hand, the model has not overfit  
244 but would benefit from more data. The model also has not underfit, which is positive and shows the potential of the model  
245 to generalize even better with more data.

246 For the diabetic retinopathy model on the EyePACS dataset, the model has not overfit and the point of convergence is  
247 roughly the same, which shows the model is almost at peak generalization. The model has seemed to underfit slightly,  
248 likely due to the complexity of the problem and the number of distinct images, along with the fact that the model was  
249 transfer learned.

### 250 3.3 Model Visualization

251 The feature importance graph is in Figure 9 for the cardiovascular risk factors model, with risk factors associated with  
252 their relative importance to the model prediction.



253

254 **Figure 9.** Relative importances of the chosen cardiovascular risk factors, represented graphically. Results obtained post-  
255 training of the random forest model.

#### 256 **4. Discussion**

257 As stated in the introduction section, there exist deep learning approaches for automatic classification of diabetic  
258 retinopathy in retinal fundus images. The average AUC ROC of the transfer-learned model presented in this study is 0.982  
259 (95% C.I., 0.980-0.984). In a study done by Google researchers classifying the same EYEPacs dataset in [13] using deep  
260 learning, an AUC ROC of 0.991 (95% C.I., 0.988-0.993) was determined [14]. In a separate study using deep learning to  
261 classify the same dataset, an AUC ROC of 0.951 (95% C.I., 0.947-0.956) was measured [17]. The model in [14] had a  
262 slightly higher AUC ROC, while that measured in [17] was significantly lower. Both models, upon trial, were not able to  
263 be implemented on the smartphone device used in this study along with several other recent smartphone models without  
264 cloud processing support due to resource needs of the complexities of the trained structures. Along with not being able to  
265 run analysis, trackage of energy and storage usage revealed significant feasibility issues on mobile devices upon trial. The  
266 model presented in this study freezes most of the trained layers in the original Inception v3 network, reducing resource-  
267 intensive complexity and allowing efficient prediction on a variety of smartphones in a rapid manner (with an average  
268 processing time of 4 seconds). In contrast to the more resource intensive models presented in [14, 17], many current  
269 smartphone-enabled approaches to automated diabetic retinopathy detection via deep learning methods have reported  
270 comparatively low accuracies. For example, in [10], a set of patients with known type 2 diabetes underwent imaging for  
271 mobile analysis. Out of these, the presence of diabetic retinopathy was only correctly detected automatically in 68.6% of  
272 patients. In comparison, the model presented in this study conducts this binary classification with 96% accuracy, and a  
273 classification of severity with above 80% accuracy. In a screening setting (with a binary classification), the device  
274 presented in this study is more effective than current methods.



275 Currently, automated cardiovascular risk prediction requires risk factors which are obtained via a blood test. A goal of this  
276 study was to remove this requirement to make risk assessment more accessible and rapid. In [11], a machine learning  
277 model was constructed to predict and identify people at risk of cardiovascular disease using 473 variables, including risk  
278 factors related to blood assays, diet and nutrition, health and medical history, family history, sociodemographic factors,  
279 psychosocial factors, physical activity, lifestyle, and physical measures. Predictive performance was assessed using the  
280 area under the receiver operating characteristic curve (AUC-ROC), which was reported to be 0.774 with a 95%  
281 Confidence Interval of 0.768-0.780. This improves on previous methods such as the Framingham score [12], however it  
282 requires many risk factors which are difficult to obtain in most regions globally. This prevents effectiveness on a large  
283 scale, especially in low-resource settings, meaning many people do not understand their risk. The model presented in this  
284 study replaces many of these risk factors with a consideration of the retinal fundus image of the patient and reports a mean  
285 AUC-ROC of 0.9 (95% CI  $\pm$  0.11). This is a statistically significant improvement. However, it is important to consider  
286 that the model presented in [11] was evaluated on data from many more participants. It is likely that the predictive  
287 performance of the model presented in this study will decrease with such a large representation, and future testing on a  
288 larger sample size must be conducted to more properly compare the models and evaluate the ability of the model  
289 presented in this study to generalize to other sub-populations. The UCI dataset is relatively small (about 1000 samples),  
290 however due to the screening nature of this application, the high cross validation accuracy, and the high AUC ROC  
291 reported above, the model remains effective in improving understanding about cardiovascular risk in an accessible, non-  
292 invasive, and quick way.

293 Xie et al. [15] found that patients with proliferative DR have an increased risk of incident cardiovascular disease, meaning  
294 that these patients must be followed up more closely to prevent cardiovascular disease. Current methods for the  
295 monitoring cardiovascular risk and diabetic retinopathy are separated, while the device presented in this study integrates

---

296 monitoring of the cardiovascular and ocular complications of diabetes, leading to improved early intervention and  
297 treatment to prevent irreversible blindness and cardiovascular disease which can lead to death. Also, due to its improved  
298 convenience, cost, speed, and non-invasiveness compared to current methods, this device has the potential to make a much  
299 broader impact, especially in developing regions and on a global scale.

## 300 **5. Conclusions**

301 The new test demonstrates performance in several metrics which compare to or surpass those of cutting-edge  
302 technologies. Current devices and tests for diabetic retinopathy require expensive machines and trained doctors, whereas  
303 this device is much cheaper (the retinal imaging attachment costs about \$30 to print), also indicating large economic  
304 profitability which would accelerate the application of this device. As well, the test is much faster (a few seconds for this  
305 test versus 2-7 weeks for current methods), meaning that early intervention is improved and that much more frequent  
306 monitoring is possible, which is lacking currently.

307 Current tests for cardiovascular risk (even automated ones) require a blood test which is expensive, invasive (which can be  
308 unsafe, especially for elderly patients or for those in regions where contamination rates are high), and time-consuming. All  
309 of these limit effective early treatment and make continuous monitoring impossible. This device instantaneously and  
310 cheaply predicts cardiovascular risk without the need for an inconvenient and invasive blood test. As well, current tests for  
311 these conditions are independent and infrequent, while in reality they should be tracked together with high frequency, due  
312 to their fundamental connectivity.

## 313 **Implementation in Developing Regions**

---

314 In communities around the world, these improvements mean that more people can easily understand and act on heart  
315 problems, saving lives across the world. Especially in developing nations, understanding complications in the heart is vital  
316 to a healthy life, and this technology shows potential to massively improve the ability of people in low-resource  
317 communities across the globe to detect and treat problems in their heart.

318 These combined, along with increased convenience and ease of use, increase the ability of this device to improve  
319 treatment for diabetic retinopathy and cardiovascular disease in developing nations. Additionally, the device facilitates  
320 continuous monitoring and remote analysis with the cloud, meaning that doctors can improve early intervention and  
321 administration of treatment even if they are not in the same region as the patient. By tracking and monitoring the  
322 progression of diabetes as it manifests in the eye and in the cardiovascular complications, we can improve early detection  
323 and intervention to detect and mitigate the complications of diabetes, even beyond the two focused on in this work. On a  
324 broader scale, this has special potential to improve the quality of medical care in developing nations with a shortage of  
325 doctors.

326 Smartphone adoption is currently relatively low in many developing regions and can vary wildly. In these settings, aid  
327 organizations can utilize this application on standard smartphones in order to screen large populations. For individual  
328 monitoring, donation to local doctors and hospitals who prescribe the devices to patients is the most effective strategy.

329 Because 3D-printing is not yet widely accessible in developing nations, at first the attachments would be cheaply printed  
330 by aid organizations and their partners for deployment in low-resource communities. We have built collaborations with  
331 such aid organizations as OneWorld Health and Microsoft 4Afrika to explore deployment of our devices in low-resource  
332 regions across Africa.

---

333 As such, the device would, at least initially, be most effective in an assistive and screening role, conveying information  
334 and prediction to doctors to enhance treatment and ability to respond early before damage is irreversible.

### 335 **Limitations**

336 Despite promising results, the device has limitations which must be addressed.

337 The field of view (FOV) of the smartphone retinal imaging attachment is limited compared to professional retinal  
338 cameras, resulting in lower descriptiveness and lower resulting accuracy. However, this can be mitigated by introducing  
339 lower-quality images into the training set, which was done in this study but should be furthered. As well, the models need  
340 to be further tested on these lower FOV retinal images to determine the extent of the lowering of accuracy.

341 Due to this limitation, currently the device is most effective as an assistive aid to be paired with a test by a professional  
342 machine, if it is necessary. However, the device is still effective for continuous monitoring and early detection to signal  
343 the need for further testing if the condition is severe.

344 Furthermore, although there was a high number of images used, they may not represent external complications which  
345 affect diagnosis, lowering model accuracy. This is especially true for the cardiovascular risk factors models, as the number  
346 of samples (~1000) was much lower than that for the diabetic retinopathy model. More data is needed for both models to  
347 improve the device in this aspect, to ensure that the models do not falter when introduced with an unknown complication.

348 Finally, some features in the dataset used were self-reported (such as years smoker, approx. cigarettes per day, and family  
349 history of diabetes), and may be biased or incorrect. Although this limitation much be acknowledged, it is inherent to most  
350 health-related datasets and is compensated for by other predictive factors.

---

351 Nonetheless, the device shows promising results and a real potential to greatly improve monitoring and early detection of  
352 diabetic retinopathy and related cardiovascular risk, improving treatment and allowing intervention before damage is  
353 irreversible in the form of complete blindness or even death. Additionally, the convenience, rapidity, non-invasiveness,  
354 and low cost of this point-of-care device allows widespread implementation in developing nations to improve the  
355 accessibility to and quality of medical care.

356

## 357 **6. Future Directions**

### 358 **6.1 Model Improvement**

359 Due to the constraint of the lack of stronger computational capabilities for this study, model size and computational power  
360 needed were important factors in determining the correct approach, which naturally came at the cost of some accuracy.

361 With extended computational resources and more time to train, this constraint would be eased, and higher model  
362 performance could be achieved. This will ensure maximum accuracy and efficiency before the models are tested in the  
363 real world. A higher number of datapoints will yield a more generalizable and therefore helpful model, so a goal of this  
364 study moving forward is the acquisition, validation, and use of more data.

365

### 366 **6.2 Preliminary Trial Feedback**

367 Another point of future work after the above steps is the gathering of data from preliminary assistive clinical trials in a  
368 closed setting where the patients are aware of the testing. This would measure the performance in a real-world system  
369 where real-world factors and noise come into play, and the effect on model performance as well as overall performance  
370 could be quantitatively as well as qualitatively measured. Potential problems with the test, the app, either model, the 3D-

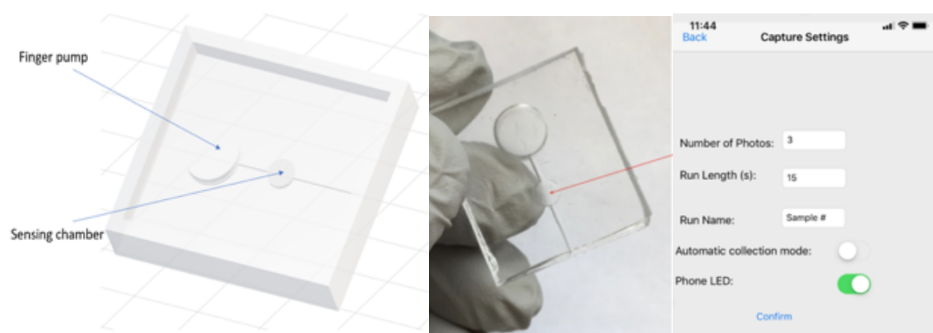
---

371 printed imaging attachment, or the deployment would be exposed and corrected before more widespread deployment.  
372 Specifically, the ability of the 3D-printed retinal imaging attachment to image a variety of distinct eyes would be  
373 evaluated. Currently, testing of this device, while present, has not been systematic to different conditions and sub-  
374 populations. This would lead to further improvement of the application based on real-world feedback. As well, both  
375 physicians and patients can slowly begin to gain trust in the system in a no-cost environment, also advancing the use of  
376 machine learning and point-of-care technologies in medicine in general.

377

### 378 **6.3 Integration with Acetone Sensor**

379 The device presented in this work intends to improve detection and monitoring of diabetic retinopathy and cardiovascular  
380 risk. Both of these conditions are related to diabetes; diabetic retinopathy is a direct complication of diabetes and diabetes  
381 has clearly been shown to be a prime risk factor for cardiovascular disease by several published studies, including [16]. In  
382 an effort to further improve early detection of diabetic retinopathy and cardiovascular disease, a novel saliva acetone  
383 sensor and accompanying smartphone app have been developed separate from this study (depicted in Figure 10).



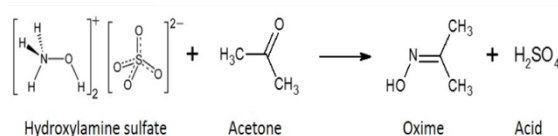
384

385 Figure 10. Left – Computer rendering of acetone sensor design, with Finger Pump and Sensing Chamber marked. Middle  
386 – Acetone sensor printed in Polydimethylsiloxane substrate. Right – Smartphone application to automatically take and  
387 analyze images.

388

389 Acetone is well-known to be directly connected to the blood glucose levels of a patient (the traditional marker for  
390 diabetes). The sensor detects acetone through observation of a chemical reaction involving acetone (Figure 11) which  
391 produces a color change in the sensing chamber. By reading the red absorbance of the sensing chamber, acetone  
392 concentration can be determined (Figure 12). Spikes in the saliva concentration of acetone are good indicators of diabetic  
393 progression and thus of diabetic complications.

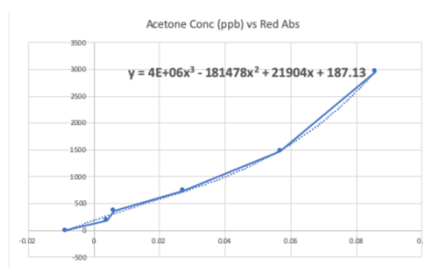
394



395

396 Figure 11. Hydroxylamine sulfate in the substrate reacts with acetone in the saliva sample, lowering the pH and triggering  
397 a color change in the pH indicator Thymol Blue.

398



399 Figure 12. Predictive curve and equation to convert red absorbance of sensing chamber to sample acetone concentration.

400

401 The implementation of this sensor, integrated with the work in this study, may improve the ability of doctors to predict  
402 diabetic complications and respond early. While initial results are promising, the device and application are currently  
403 undergoing more comprehensive evaluation to measure sensitivity, accuracy, and potential issues.

404

#### 405 Acknowledgement of Role of Funding Source

406 No external funding source to declare.

407  
408 **7. Summary**

409 The goal of this work was to create an integrated test, automated and not requiring laboratory blood analysis, for screening  
410 for diabetic retinopathy and cardiovascular risk. First, a random forest model was developed by retrospectively analyzing  
411 the influence of various risk factors (obtained quickly and non- invasively) on cardiovascular risk. Next, a deep-learning  
412 model was developed for prediction of diabetic retinopathy from retinal fundus images by transfer learning the  
413 InceptionV3 model and pre-processing the images via automatic vessel segmentation. The models were integrated into a  
414 smartphone-based device, combined with an inexpensive 3D-printed retinal imaging attachment. Accuracy scores, as well  
415 as the receiver operating characteristic curve, the learning curve, and other gauges, were promising. This test is much  
416 cheaper and faster, enabling continuous monitoring for diabetes and its complications. It has the potential to replace the  
417 manual methods of diagnosing both diabetic retinopathy and cardiovascular risk, which are time consuming and costly  
418 processes only done by medical professionals away from the point of care, and to prevent irreversible blindness and heart-  
419 related complications through faster, cheaper, and safer monitoring of diabetes. Tracking of cardiovascular and ocular  
420 complications of diabetes can also enable improved detection of other diabetic complications, leading to earlier and more  
421 efficient treatment on a global scale.

422  
423 **8. References**

- 424 1. G. Azzopardi, N. Strisciuglio, M. Vento, N. Petkov, Trainable cosfire filters for vessel delineation with application  
425 to retinal images, *Medical image analysis* 19 (2015) 46–57
- 426 2. J.J. Staal, M.D. Abramoff, M. Niemeijer, M.A. Viergever, B. van Ginneken, "Ridge based vessel segmentation in  
427 color images of the retina", *IEEE Transactions on Medical Imaging*, 2004, vol. 23, pp. 501-509.
- 428 3. Cuadros J, Bresnick G. EyePACS: An Adaptable Telemedicine System for Diabetic Retinopathy Screening. *Journal*  
429 *of diabetes science and technology* (Online). 2009;3(3):509-516
- 430 4. Lam C, Yi D, Guo M, Lindsey T. Automated Detection of Diabetic Retinopathy using Deep Learning. *AMIA Jt*  
431 *Summits Transl Sci Proc.* 2018;2017:147-155. Published 2018 May 18
-



- 432 5. Jan Odstrcilik, Jiri Jan, Radim Kolar, and Jiri Gazarek. Improvement of vessel segmentation by matched filtering in  
433 colour retinal images. In IFMBE Proceedings of World Congress on Medical Physics and Biomedical Engineering,  
434 pages 327 - 330, 2009.
- 435 6. A. Hoover, V. Kouznetsova and M. Goldbaum, "Locating Blood Vessels in Retinal Images by Piece-wise Threhsold  
436 Probing of a Matched Filter Response", *IEEE Transactions on Medical Imaging* , vol. 19 no. 3, pp. 203-210, March  
437 2000.
- 438 7. Heart Disease Facts & Statistics. (n.d.). Retrieved from <https://www.cdc.gov/heartdisease/facts.html>
- 439 8. Facts About Diabetic Eye Disease. (2015, September 01). Retrieved from  
440 <https://nei.nih.gov/health/diabetic/retinopathy>
- 441 9. Janosi, Andreas & Steinbrunn, William & Pfisterer, Mathias & Detrano, Robert. *Heart Disease Dataset*. UCI.  
442 archive.ics.uci.edu/ml/datasets/heart+Disease
- 443 10. Rajalakshmi, R., Subashini, R., Anjana, R. M., & Mohan, V. (2018). Automated diabetic retinopathy detection in  
444 smartphone-based fundus photography using artificial intelligence. *Eye (London, England)*, 32( 6), 1138–1144.  
445 <https://doi.org/10.1038/s41433-018-0064-9>
- 446 11. Alaa, A. M., Bolton, T., Di Angelantonio, E., Rudd, J., & van der Schaar, M. (2019). Cardiovascular disease risk  
447 prediction using automated machine learning: A prospective study of 423,604 UK Biobank participants. *PloS one*, 14  
448 (5), e0213653. <https://doi.org/10.1371/journal.pone.0213653>
- 449 12. Jahangiry, L., Farhangi, M. A., & Rezaei, F. (2017). Framingham risk score for estimation of 10-years of  
450 cardiovascular diseases risk in patients with metabolic syndrome. *Journal of health, population, and nutrition*, 36(1),  
451 36. <https://doi.org/10.1186/s41043-017-0114-0>
- 452 13. Kaggle Diabetic Retinopathy Detection competition. <https://www.kaggle.com/c/diabetic-retinopathy-detection>.  
453 Accessed November, 2018.
- 454 14. Gulshan V, Peng L, Coram M, et al. Development and Validation of a Deep Learning Algorithm for Detection of  
455 Diabetic Retinopathy in Retinal Fundus Photographs. *JAMA*. 2016;316(22):2402–2410.  
456 doi:10.1001/jama.2016.17216
- 457 15. Xie J, Ikram MK, Cotch MF, et al. Association of diabetic macular edema and proliferative diabetic retinopathy with  
458 cardiovascular disease: a systematic review and meta-analysis. *JAMA Ophthalmol*. 2017;135:586-593.
- 459 16. Dokken, B. (2008). The Pathophysiology of Cardiovascular Disease and Diabetes: Beyond Blood Pressure and Lipids.  
460 *Diabetes Spectrum*. Jul 2008, 21 (3) 160-165; DOI: 10.2337/diaspect.21.3.160
- 461 17. Voets, M., Møllersen, K., & Bongo, L. A. (2019). Reproduction study using public data of: Development and  
462 validation of a deep learning algorithm for detection of diabetic retinopathy in retinal fundus photographs. *PloS*  
463 *one*, 14(6), e0217541. <https://doi.org/10.1371/journal.pone.0217541>
- 464
-